Analysis of Graphene Quantum Dots as Energy Storage Systems Using DFT

1st Tharles A. Ribeiro
School of Electrical and Computer Engineering
State University of Campinas
Campinas - SP, Brazil
tharlesmg@gmail.com

2nd Renato G. Freitas
Department of Chemistry
Federal University of Mato Grosso
Cuiabá - MT, Brazil

3rd Hudson Zanin
Carbon Sci-Tech Labs
State University of Campinas
Campinas - SP, Brazil
hzanin@unicamp.br

***Abstract*—Following Climate action conference 28, there has been a notable surge in the demand for more efficient energy storage devices. Supercapacitors and batteries are emerging as promising alternatives due to their low cost, long cycle life, high power density, and excellent cycling stability. These attributes make them suitable for both conventional applications and integration into renewable energy systems and smart grids, contributing significantly to the global energy transition. Nanostructured materials, such as graphene quantum dots, have emerged as promising candidates due to their unique properties, including high surface area, exceptional electrical conductivity, structural stability, ease of manufacturing and functionalization, and environmental compatibility. This study investigates the electronic and optical properties resulting from the intercalation of different species of monovalent ions between two graphene quantum dots with hydrogenated edges, using Density Functional Theory - based simulations. Simulations were conducted with Gaussian 09 software, employing the CAM-B3LYP functional and a 6-311++G(d,p) basis set. Raman spectroscopy results show shifts in the D and G bands for graphene quantum dots intercalated with lithium, sodium, potassium, fluorine, chlorine, and bromine ions. Positive ions generally induce a red shift in the Raman bands, whereas negative ions lead to a blue shift. Disorder ratios derived from Raman spectra suggest increased structural defects with positive ions and a mitigated effect with negative ions. Adsorption energy calculations reveal that lithium ions exhibit the highest interaction with graphene quantum dots, while fluorine shows the strongest bonding among anions. Analysis of the Highest Occupied Molecular Orbital and Lowest Unoccupied Molecular Orbital reveals that the presence of positive ions on the surface of graphene quantum dots increases the electronic density in that region. Conversely, negative ions cause the electronic density to concentrate around the ion. This indicates that graphene quantum dots have an enhanced ability to donate and accept electrons. The high electronic density of graphene quantum dots enhances the efficiency of energy storage and release, making them promising nanostructured solutions for energy storage systems. These attributes underscore the importance of studying graphene quantum dots for the development of more efficient devices. Consequently, graphene quantum dots play a significant role in the energy transition and environmental protection.**

***Index Terms*—Adsorption, Energy Storage, Graphene, Quantum dots, Raman**

I. Introduction

After COP 28, there has been a significant increase in demand for more efficient energy storage devices than the current ones. In this context, supercapacitors emerge as ideal alternatives due to their low cost, long cycle life, high power density, and outstanding cycling stability. [1] [2] [3] [4] These characteristics make them promising not only for conventional applications but also for integrating renewable energy systems and smart grids, thereby contributing to global energy transition.

To achieve greater efficiency, the choice of electrode material has a direct impact on the electrochemical properties of the device. Additionally, the material must be capable of optimizing storage capacity, charge, and discharge, while ensuring long-term energy efficiency. Therefore, exploring new materials is crucial for the development of high-performance energy storage devices. In this context, nanostructured materials, such as graphene, stand out as promising candidates. [5]

In the current context, nanostructured materials such as graphene quantum dots (GQDs) emerge as a promising option to meet the increasing demand for advanced energy storage solutions. GQDs exhibit a range of distinct characteristics that make them particularly suitable for applications in supercapacitors and other next-generation energy storage devices. [6]

Among these characteristics, notable features include the remarkable surface area, which significantly enhances the electrical charge storage capacity, graphene's exceptional electrical conductivity that allows efficient electron transfer during charge and discharge processes, robust structural stability ensuring durability and resistance to repeated cycles, ease of manufacturing and functionalization enabling precise adjustments to material properties as required by specific applications, and environmental compatibility, promoting sustainable practices in energy storage technology production. [6] [7] [8]

For the synthesis of graphene quantum dots (GQDs), there are two main techniques. The top-down technique uses carbon-based materials of larger dimensions such as graphite, graphene oxide, and graphene as initial resources to achieve a carbon-based nanomaterial solution through chemical or physical methods. These include laser ablation, chemical oxidation, chemical exfoliation, arc discharge, and ultrasonication. [9] [10] [11] [12] Conversely, the bottom-up technique utilizes smaller carbon-based molecules to generate GQDs through methods such as hydrothermal, microwave, and pyrolysis. [13] [14]

This study focuses on investigating the electronic properties in the energy storage process and its optical consequences

resulting from the intercalation of different species of monovalent ions between two graphene quantum dots with hydrogenated edges, using simulations based on Density Functional Theory (DFT).

II. Methodology

For this study, all simulations were performed using Gaussian 09 softwares, employing Density Functional Theory (DFT) methodology. [15] [16] [17]. Initially, a graphene sheet was optimized in vacuum using the CAM-B3LYP exchange-correlation functional and a 6-311++G(d,p) basis set. [17] [18] After optimizing the initial geometry of the graphene sheet, it was duplicated and stacked face-to-face to form the structure of two graphene quantum dots, which was then re-optimized.

Subsequently, lithium, sodium, potassium, fluorine, chlorine, and bromine ions were individually added to the GQDs, resulting in structures labeled as GQD@Li^+, GQD@Na^+, GQD@K^+, GQD@F^-, GQD@Cl^-, and GQD@Br^-. After each ion addition, the simulations were re-optimized to compute vibrational frequencies and subjected to DFT quantum mechanics calculations at the CAM-B3LYP/6-311++G(d,p) level.

During geometry optimization, it was observed that there were no imaginary frequency modes, indicating that the simulations reached minimum energy points. To correlate theoretical results with experimental data, scaling factors were adjusted using a correction factor. [19]

Starting from the optimized simulations, results from Raman spectroscopy were obtained, including analysis of the D and G bands, as well as the electronic structure of the systems under study.

The intensity ratios between the D and G modes are a significant characteristic of graphene structures. Specifically, the

$$ID/IG \tag{1}$$

where ID and IG represent the intensities of the D and G bands, respectively, is a crucial parameter related to the defect density in the graphene crystal lattice. [20]

From the optimization, the total adsorption energy ΔE_{ads} was calculated for each structure according to the equation:

$$\Delta E_{ads} \equiv E_{x+\#G^-}(E_G + E_x) \tag{2}$$

Where $E_{x+\#G}$ is the total energy of each structure after ionic adsorption, EG is the total energy of isolated graphene structures and Ex+ corresponds to the ion's total energy.

The Highest Occupied Molecular Orbital (HOMO) and Lowest Unoccupied Molecular Orbital (LUMO) were simulated using the same functional and basis set for each ion-GQD system, providing a detailed characterization of the electronic and structural properties of these materials.

III. Results and Discussion

Raman spectroscopy is an essential technique for investigating the properties of carbon nanostructures, such as their structure and electronic characteristics. [21] [22] In the context of graphene, the main observed bands are: the G band (1580 cm^{-1}), which reflects the planar vibration of sp2 carbon atoms in the graphene structure; the D band (1200–1350 cm^{-1}), associated with structural defects and localized perturbations near defects or edges of graphene, representing "breathing" motions of the carbon rings. [23] [24] [21] [24] [25] [26] In this study, we focus on analyzing the interference caused by the presence of monovalent ions in the graphene structure.

In Figure 1, the Raman spectroscopy results obtained for pure graphene quantum dots and for GQDs intercalated with

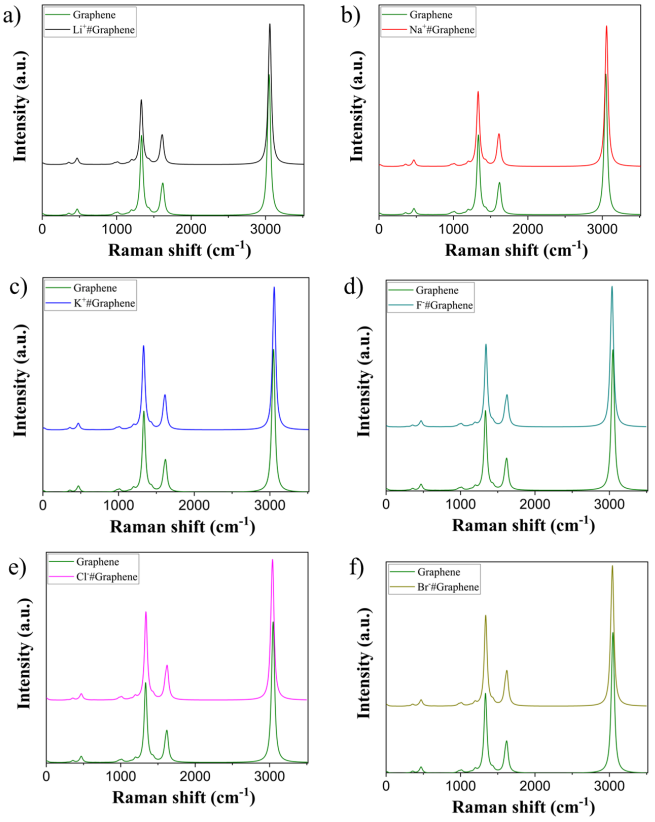

Fig. 1. Frequency Raman Spectrum for (a) GQD, (b) GQD@Li, (c) GQD@Na^+, (d) GQD@k^+, (e) GQD@F^-, (f) GQD@Cl^-, (g) GQD@Br^-.

lithium, sodium, potassium, fluorine, chlorine, and bromine ions were analyzed through Raman frequencies.

In the D band (Figure 2a) and G band (Figure 2b). For the pure quantum dot without ion presence, the D band was calculated at 1334.65 cm^{-1} and the G band at 1615.23 cm^{-1}. For the lithium ion, frequencies were measured at 1331.28 cm^{-1} for the D band and 1608.73 cm^{-1} for the G band, showing shifts of -3.4 cm^{-1} and -7.17 cm^{-1}, respectively, compared to pure graphene, indicating a red shift. Sodium ion measurements showed frequencies of 1331.30 cm^{-1} for

the D band and 1609.41 cm^{-1} for the G band, with shifts of -3.34 cm^{-1} and -6.43 cm^{-1}, respectively, relative to pure graphene, also indicating a red shift in the D band. Potassium ion simulations revealed frequencies of 1331.0 cm^{-1} for the D band and 1610.43 cm^{-1} for the G band, with shifts of -3.64 cm^{-1} and -5.23 cm^{-1}.

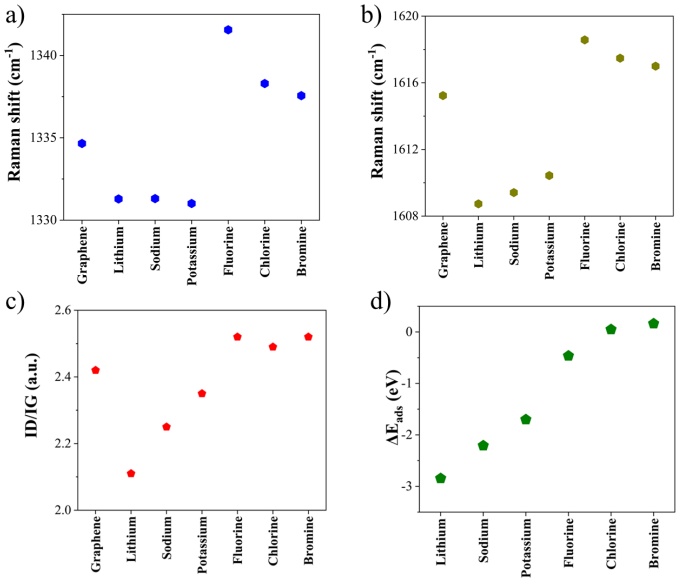

Fig. 2. (a) Raman Shift D band, (b) Raman Shift G band, (c) Adsorption Energy, (d) IG/ID

For fluorine intercalated GQDs, the frequencies were 1341.55 cm^{-1} in the D band and 1618.57 cm^{-1} in the G band. For chlorine ions, frequencies were found to be 1338.29 cm^{-1} in the D band and 1617.47 cm^{-1} in the G band. Finally, bromine ions exhibited frequencies of 1337.55 cm^{-1} in the D band and 1617.0 cm^{-1} in the G band. In general, the D and G bands for Li, Na, and K models are red-shifted, whereas the D bands for F, Cl, and Br are blue-shifted.

In Figure 2c, the disorder ratios were calculated as the ratio between the peak of the D band and the G band. For pure graphene, the disorder ratio was 2.42. Notably, lithium, sodium, and potassium ions exhibited higher disorder ratios compared to pure graphene, with values of 2.11, 2.25, and 2.35, respectively. These results suggest an increase in structural defects or perturbations in the crystal lattice induced by ion intercalation. In contrast, fluorine, chlorine, and bromine ions showed slightly lower disorder ratios compared to the pure graphene quantum dot, with values of 2.52, 2.49, and 2.25, respectively. This behavior may indicate a potential mitigation of structural disorder effects introduced by ions, highlighting distinct modifications in the electronic structure and organization of intercalated graphene quantum dots.

In Figure 2d, the adsorption energy calculated using Equation 1 is highlighted. The adsorption energy was determined for each ionic species. For lithium ion intercalated with two GQDs, an energy of -2.84 eV was found. For sodium ion, the adsorption energy was -2.21 eV; for potassium ion, it was -1.70 eV; for fluorine, the adsorption energy was -0.46 eV; for chlorine, it was 0.05 eV; and for bromine, it was 0.16 eV. It was observed that lithium ion exhibited a higher adsorption energy compared to sodium and potassium ions, indicating a more intense electrostatic interaction due to lithium's higher nuclear charge and smaller ionic radius. This interaction implies that lithium ion is more strongly attracted to the surface of GQDs compared to sodium and potassium ions.

Among the anions, fluorine showed a higher adsorption energy compared to chlorine and bromine. This suggests that fluorine forms a stronger bond with GQDs, possibly due to its lower polarizability and smaller size, which facilitates closer interaction with GQD surfaces.

In Figure 3 and 4, the frontier molecular orbitals (HOMO and LUMO) and their isolines are displayed, allowing visualization of two primary levels: the first, commonly known as the Highest Occupied Molecular Orbital, and the other designated as the Lowest Unoccupied Molecular Orbital, for pure graphene (Fig.4a), with lithium (Fig.4b), sodium (Fig.4c), potassium (Fig.4d) and fluorine (Fig.5a), chlorine (Fig.5b), bromine (Fig.5c) ions intercalated between the GQDs.

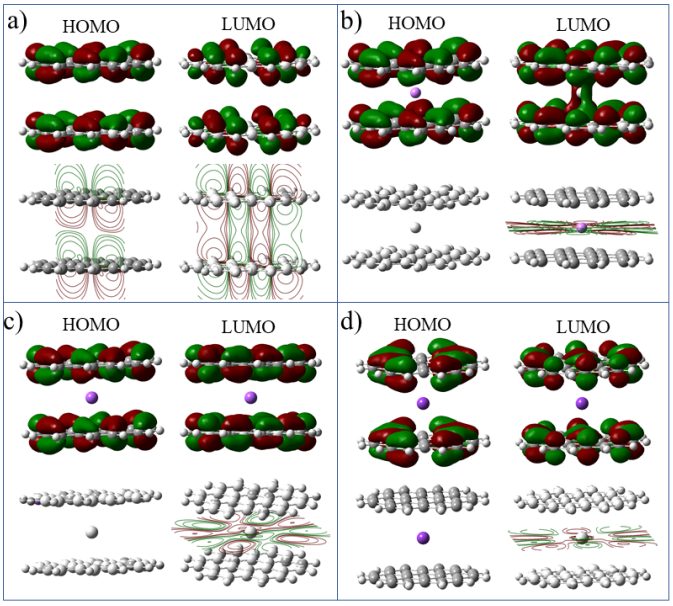

Fig. 3. Orbitals and isolines of (a) GQD, (b) GQD@Li^+, (c) GQD@Na^+, (d) GQD@K^+.

The electronic density surface for the HOMO orbital of the graphene surface without an ion exhibits a uniform distribution of electronic density across the surface. However, the electronic density is lower near the positive ion in the electronic density surface for the HOMO orbital of the graphene surface with a nearby positive ion. Conversely, the electronic density surface for the HOMO orbital of the graphene surface with a nearby negative ion shows a higher electronic density region near the ion.

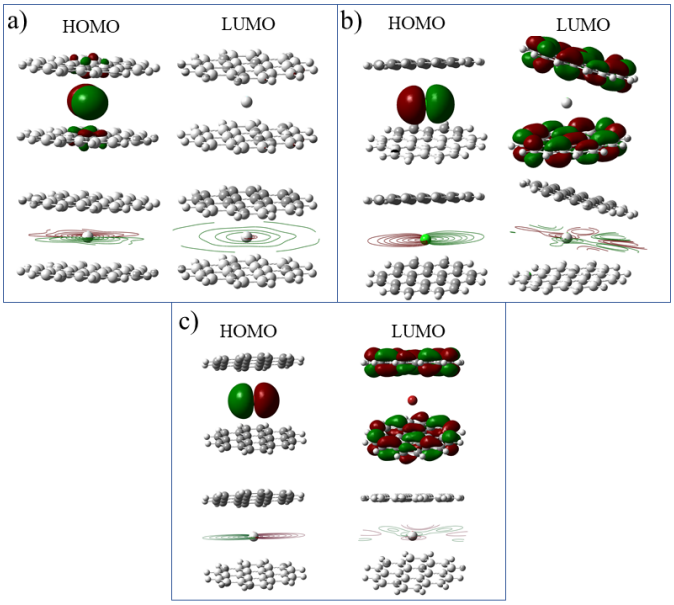

Fig. 4. Orbitals and isolines of (a) GQD@F^-, (b) GQD@Cl^-, (c) GQD@Br^-.

The analysis of the electron density isosurfaces for the LUMO orbitals shows a similar pattern. The electron density isosurface for the LUMO orbital of the graphene surface without ions exhibits a uniform distribution of electron density across the surface. However, the electron density isosurface for the LUMO orbital of the graphene surface with a nearby positive ion shows a region of higher electron density near the ion, whereas the electron density isosurface for the LUMO orbital of the graphene surface with a nearby negative ion shows a region of lower electron density near the ion and higher density on the GQD surface

IV. Conclusion

Based on the detailed results of Raman spectroscopic analysis, adsorption energy, and density of states of graphene quantum dots functionalized with different alkali and halogen ions, it is concluded that these materials undergo substantial changes in their structural and electronic properties upon ion intercalation. Raman spectroscopy revealed that ions such as lithium, sodium, and potassium cause red shifts in the frequencies of the D and G bands, indicative of modifications in the graphene's crystalline structure. In contrast, halogens such as fluorine, chlorine, and bromine resulted in blue shifts in the D band, reflecting changes in the electronic structure of graphene.

The analysis of the adsorption energy of ions on graphene quantum dots reveals promising results for their application in energy storage systems, where this material can function as cathodes or anodes depending on its structure and functionalization. The obtained data indicate that lithium exhibits the highest adsorption energy, with a value of -2.84 eV, suggesting a strong interaction between lithium and the GQD surface. This robust interaction may potentially enhance charge transfer efficiency during the battery's charging and discharging processes. Sodium also demonstrates significant performance, presenting an adsorption energy of -2.21 eV, while potassium, with -1.70 eV, shows a less favorable interaction, although still relevant. These negative values indicate that both lithium and sodium are promising candidates for cathode function, as they provide a high capacity for energy storage.

In contrast, when considering anions, the results are less encouraging. Fluorine exhibits a positive adsorption energy of 0.46 eV, followed by bromine at 0.16 eV and chlorine at 0.05 eV. These values suggest that halogens are not ideal for anode function, as the less favorable interactions may compromise the efficiency and stability of the energy storage system. The lower affinity of anions for GQDs could result in reduced energy storage capacity and instability during the charge and discharge cycles.

Therefore, these results indicate significant potential for GQDs as advanced materials in energy storage technologies, providing a solid foundation for further studies focused on optimizing performance, durability, and efficiency of these materials in practical applications. Continued research in this field is crucial to fully exploit the potential of these materials and drive the development of more efficient and sustainable energy storage devices.

References

[1] Z. Zhang, F. Xiao, L. Qian, J. Xiao, S. Wang, and Y. Liu, "Facile synthesis of 3d mno2–graphene and carbon nanotube–graphene composite networks for high-performance, flexible, all-solid-state asymmetric supercapacitors," *Advanced Energy Materials*, vol. 4, no. 10, p. 1400064, 2014.

[2] P. Cai, R. Momen, M. Li, Y. Tian, L. Yang, K. Zou, X. Deng, B. Wang, H. Hou, G. Zou *et al.*, "Functional carbon materials processed by nh3 plasma for advanced full-carbon sodium-ion capacitors," *Chemical Engineering Journal*, vol. 420, p. 129647, 2021.

[3] K. Zou, P. Cai, X. Deng, B. Wang, C. Liu, J. Li, H. Hou, G. Zou, and X. Ji, "Revealing dual capacitive mechanism of carbon cathode toward ultrafast quasi-solid-state lithium ion capacitors," *Journal of Energy Chemistry*, vol. 60, pp. 209–221, 2021.

[4] P. Cai, K. Zou, X. Deng, B. Wang, M. Zheng, L. Li, H. Hou, G. Zou, and X. Ji, "Comprehensive understanding of sodium-ion capacitors: definition, mechanisms, configurations, materials, key technologies, and future developments," *Advanced Energy Materials*, vol. 11, no. 16, p. 2003804, 2021.

[5] X. Deng, K. Zou, R. Momen, P. Cai, J. Chen, H. Hou, G. Zou, and X. Ji, "High content anion (s/se/p) doping assisted by defect engineering with fast charge transfer kinetics for high-performance sodium ion capacitors," *Science Bulletin*, vol. 66, no. 18, pp. 1858–1868, 2021.

[6] J. Xiao, R. Momen, and C. Liu, "Application of carbon quantum dots in supercapacitors: a mini review," *Electrochemistry Communications*, vol. 132, p. 107143, 2021.

[7] R. Guo, L. Li, B. Wang, Y. Xiang, G. Zou, Y. Zhu, H. Hou, and X. Ji, "Functionalized carbon dots for advanced batteries," *Energy Storage Materials*, vol. 37, pp. 8–39, 2021.

[8] L. Li, Y. Li, Y. Ye, R. Guo, A. Wang, G. Zou, H. Hou, and X. Ji, "Kilogram-scale synthesis and functionalization of carbon dots for superior electrochemical potassium storage," *ACS nano*, vol. 15, no. 4, pp. 6872–6885, 2021.

[9] G. Chen, S. Wu, L. Hui, Y. Zhao, J. Ye, Z. Tan, W. Zeng, Z. Tao, L. Yang, and Y. Zhu, "Assembling carbon quantum dots to a layered carbon for high-density supercapacitor electrodes," *Scientific reports*, vol. 6, no. 1, p. 19028, 2016.

[10] S. Ahirwar, S. Mallick, and D. Bahadur, "Electrochemical method to prepare graphene quantum dots and graphene oxide quantum dots," *ACS omega*, vol. 2, no. 11, pp. 8343–8353, 2017.
[11] S. Kang, Y. K. Jeong, K. H. Jung, Y. Son, W. R. Kim, J. H. Ryu, and K. M. Kim, "One-step synthesis of sulfur-incorporated graphene quantum dots using pulsed laser ablation for enhancing optical properties," *Optics Express*, vol. 28, no. 15, pp. 21 659–21 667, 2020.
[12] S. Kang, Y. K. Jeong, J. H. Ryu, Y. Son, W. R. Kim, B. Lee, K. H. Jung, and K. M. Kim, "Pulsed laser ablation based synthetic route for nitrogen-doped graphene quantum dots using graphite flakes."
[13] M. Wu, Y. Wang, W. Wu, C. Hu, X. Wang, J. Zheng, Z. Li, B. Jiang, and J. Qiu, "Preparation of functionalized water-soluble photoluminescent carbon quantum dots from petroleum coke," *Carbon*, vol. 78, pp. 480–489, 2014.
[14] M. Li, C. Yu, C. Hu, W. Yang, C. Zhao, S. Wang, M. Zhang, J. Zhao, X. Wang, and J. Qiu, "Solvothermal conversion of coal into nitrogen-doped carbon dots with singlet oxygen generation and high quantum yield," *Chemical Engineering Journal*, vol. 320, pp. 570–575, 2017.
[15] M. J. Frisch, G. W. Trucks, H. B. Schlegel, G. E. Scuseria, M. A. Robb, J. R. Cheeseman, G. Scalmani, V. Barone, G. A. Petersson, H. Nakatsuji, X. Li, M. Caricato, A. V. Marenich, J. Bloino, B. G. Janesko, R. Gomperts, and B. Mennucci, "Gaussian˜09 Revision C.01," 2016, gaussian Inc. Wallingford CT.
[16] W. Kohn and L. J. Sham, "Self-consistent equations including exchange and correlation effects," *Physical review*, vol. 140, no. 4A, p. A1133, 1965.
[17] M. J. Frisch, J. A. Pople, and J. S. Binkley, "Self-consistent molecular orbital methods 25. supplementary functions for gaussian basis sets," *The Journal of chemical physics*, vol. 80, no. 7, pp. 3265–3269, 1984.
[18] T. Yanai, D. P. Tew, and N. C. Handy, "A new hybrid exchange–correlation functional using the coulomb-attenuating method (cam-b3lyp)," *Chemical physics letters*, vol. 393, no. 1-3, pp. 51–57, 2004.
[19] D. Kashinski, G. Chase, R. Nelson, O. Di Nallo, A. Scales, D. VanderLey, and E. Byrd, "Harmonic vibrational frequencies: approximate global scaling factors for tpss, m06, and m11 functional families using several common basis sets," *The Journal of Physical Chemistry A*, vol. 121, no. 11, pp. 2265–2273, 2017.
[20] A. C. Ferrari and D. M. Basko, "Raman spectroscopy as a versatile tool for studying the properties of graphene," *Nature nanotechnology*, vol. 8, no. 4, pp. 235–246, 2013.
[21] T. T. Tung, A. L. Pereira, E. Poloni, M. N. Dang, J. Wang, T.-S. D. Le, Y.-J. Kim, Q. H. Pho, M. J. Nine, C. J. Shearer *et al.*, "Irradiation methods for engineering of graphene related two-dimensional materials," *Applied Physics Reviews*, vol. 10, no. 3, 2023.
[22] J. Liu, Q. Li, Y. Zou, Q. Qian, Y. Jin, G. Li, K. Jiang, and S. Fan, "The dependence of graphene raman d-band on carrier density," *Nano Letters*, vol. 13, no. 12, pp. 6170–6175, 2013, pMID: 24283411. [Online]. Available: https://doi.org/10.1021/nl4035048
[23] Y. Y. Wang, Z. H. Ni, T. Yu, Z. X. Shen, H. M. Wang, Y. H. Wu, W. Chen, and A. T. Shen Wee, "Raman studies of monolayer graphene: the substrate effect," *The Journal of Physical Chemistry C*, vol. 112, no. 29, pp. 10 637–10 640, 2008.
[24] G. Compagnini, G. Forte, F. Giannazzo, V. Raineri, A. La Magna, and I. Deretzis, "Ion beam induced defects in graphene: Raman spectroscopy and dft calculations," *Journal of Molecular Structure*, vol. 993, no. 1-3, pp. 506–509, 2011.
[25] J.-B. Wu, M.-L. Lin, X. Cong, H.-N. Liu, and P.-H. Tan, "Raman spectroscopy of graphene-based materials and its applications in related devices," *Chemical Society Reviews*, vol. 47, no. 5, pp. 1822–1873, 2018.
[26] L. M. Malard, M. A. Pimenta, G. Dresselhaus, and M. S. Dresselhaus, "Raman spectroscopy in graphene," *Physics reports*, vol. 473, no. 5-6, pp. 51–87, 2009.